

# 1 Identifying the dynamic contact 2 network of infectious disease spread

3 Pratha Sah<sup>1</sup> and Shweta Bansal<sup>1\*</sup>

\*For correspondence:

[shweta.bansal@georgetown.edu](mailto:shweta.bansal@georgetown.edu)  
(SB)

4 <sup>1</sup>Department of Biology, Georgetown University, Washington, DC

---

## 6 Abstract

7 Pathogen propagation is a fundamental process that takes place through host contact networks.  
8 While it has been possible to characterize contact networks of several human infectious diseases  
9 (e.g., sexual contacts for HIV, physical proximity for measles), logistical difficulties and the high costs  
10 of data collection makes network modeling of infectious diseases in animal populations particularly  
11 difficult. In addition, limited knowledge about how pathogens transmit precludes an accurate  
12 definition of network edges required for constructing networks of disease transmission. We  
13 developed a new tool, INoDS (Identifying Networks of infectious Disease Spread), that utilizes  
14 Bayesian inference to provide evidence towards the underlying contact network of an infectious  
15 disease spread. We show that the tool accurately identifies the underlying contact network even  
16 when the networks are partially sampled and information on disease spread is incomplete. We  
17 next demonstrate the applicability of the tool in two real animal populations: bumble bees and  
18 Australian sleepy lizards. The performance of INoDS in synthetic and complex empirical systems  
19 highlights its role as an alternative approach to laboratory transmission experiments, in providing  
20 epidemiological insights into novel and less known host-pathogen systems, and overcoming  
21 common data-collection constraints.

---

## 23 Introduction

24 Host contacts, whether direct or indirect, play a fundamental role in the spread of infectious disease  
25 through host populations (*Sah et al., 2017*). Traditional epidemiological models, however make  
26 simplistic assumptions such as homogeneous mixing of individuals, no social structure, which  
27 are often unrealistic and in many cases yield unreliable predictions of disease spread (*Bansal  
28 et al., 2007*). Therefore, in recent years, the network approach to modeling infection spread has  
29 gained popularity because it explicitly incorporates host interactions that mediate infection spread.  
30 Formally, in a contact network model, individuals are represented as nodes, and an edge between  
31 two nodes represents an interaction that has the potential to transmit the infection. An exact  
32 contact network model requires (i) knowledge of the transmission mechanism of the spreading  
33 pathogen (required to define an edge in contact network), (ii) data on all individuals in a population,  
34 and (iii) all disease-causing interactions between the individuals. In addition, the accuracy of disease  
35 predictions depends on the knowledge of epidemiological characteristics of the spreading infection,  
36 including the rate of transmission given a contact between two individuals and the rate of recovery  
37 of infected individuals. The use of modern technology in recent years, including RFID tags, GPS,  
38 radio tags, proximity logger and automated video tracking has enabled the collection of detailed  
39 movement and contact data, making network modeling feasible.

40 Despite the technology, logistical and financial constraints still prevent data-collection of each  
41 individual and each interaction occurring in a host population (*Welch et al., 2011; Godfrey, 2013*).  
42 More importantly, limited knowledge about the pathogen makes it challenging to identify the mode

43 of infection transmission, and a disease causing contact between individuals. Laboratory techniques  
44 of unraveling transmission mechanisms usually take years to resolve. Defining accurate contact  
45 networks underlying infection transmission in human infectious disease has been far from trivial  
46 (*Bansal et al., 2007*). For animal infectious disease, limited knowledge about host behavior along  
47 with the characteristics of the spreading pathogen makes it particularly difficult to define an exact  
48 contact network, which has severely limited the scope of network modeling in animal and wildlife  
49 epidemiology (*Craft and Caillaud, 2011*).

50 Lack of knowledge about host-pathogen characteristics has prompted the use of several indirect  
51 approaches to identify the link between network structure of animal societies and disease spread. A  
52 popular approach has been to explore the relation between social network position on disease risk  
53 (*Godfrey et al., 2009, 2010; MacIntosh et al., 2012*). However, this approach can be misleading as the  
54 position of individuals in social networks depends on dominance hierarchy, age, sex, reproductive  
55 status, and can be very different from their position in a contact network that is relevant to infection  
56 transmission. Another approach is to use proxy networks, such as movement networks, and  
57 network based on spatial proximity or home-range overlap, as a surrogate to all direct and indirect  
58 contacts between individuals (*Danon et al., 2011; Hamede et al., 2009; Fenner et al., 2011*). A recent  
59 approach, called the *k*-test procedure, explores a direct link between infectious disease spread  
60 and contact network by comparing the number of infectious contacts of infected cases to that of  
61 uninfected cases (*VanderWaal et al., 2016*).

62 However, several challenges still remain in identifying the underlying contact networks of  
63 infection spread in a host population. First, it is often unclear how edge weights (whether duration,  
64 frequency or intensity) relate to transmission risk unless validated by transmission-experiments  
65 (*Aiello et al., 2016*). Furthermore, the relevance of low-weighted edges in a contact network is  
66 ambiguous (*Pellis et al., 2014*). The interaction network of any social group will appear as a fully  
67 connected network if monitored for a long period of time. As fully-connected contact networks rarely  
68 reflect the transmission of an infection through a population, one may ask whether low weighted  
69 links can be ignored, and what constitutes an edge-weight threshold below which interactions are  
70 epidemiologically irrelevant? Second, many previous approaches ignore the dynamic nature of host  
71 contacts. The temporal evolution of contacts between hosts, however is crucial in determining the  
72 order in which contacts occur, which regulates the spread of an infectious disease spread through  
73 the host population (*Bansal et al., 2010*). Therefore, a static representation of host interactions  
74 often serves as an inferior contact network model because it fails to approximate disease spread  
75 through dynamic host networks (*Fefferman and Ng, 2007; Farine, 2017*). Third, an approach that  
76 establishes the predictive power of a network to describe the dynamics of disease spread is lacking.  
77 Although spatial proximity or home-range overlap as proxies for infectious contact may be a  
78 reasonable assumption to make considering the limited data that is available for certain wildlife  
79 systems, such contact network models may be uninformative. This is because, by mixing disease-  
80 spreading contacts with those that are epidemiologically irrelevant, the disease predictions from  
81 such networks may not be reliable or accurate. Finally, to our knowledge, none of the previous  
82 approaches allow testing of competing hypotheses about disease transmission mechanisms which  
83 (may) generate distinct contact patterns and consequently different contact network models.

84 All of these challenges demand the need of an approach that can allow hypothesis testing  
85 between different contact network models while taking into account the dynamics of animal  
86 interactions and missing data due to incomplete network sampling. In this study, we introduce a  
87 computational tool called INoDS (*I*dentifying *N*etworks of infectious *D*isease *S*pread) that utilizes  
88 Bayesian inference to identify the underlying contact network of disease transmission in host  
89 populations. Our tool can infer contact networks of a wide range of infectious disease types (SI, SIS,  
90 and SIR) and can be easily extended for complex disease spread models. We develop a three-step  
91 approach to enable power analysis and hypothesis testing on contact network models of infectious  
92 disease spread (Figure. 1). Our tool provides inference on dynamic and static contact network  
93 models, and is robust to common forms of missing data. Using two real-world datasets, we highlight

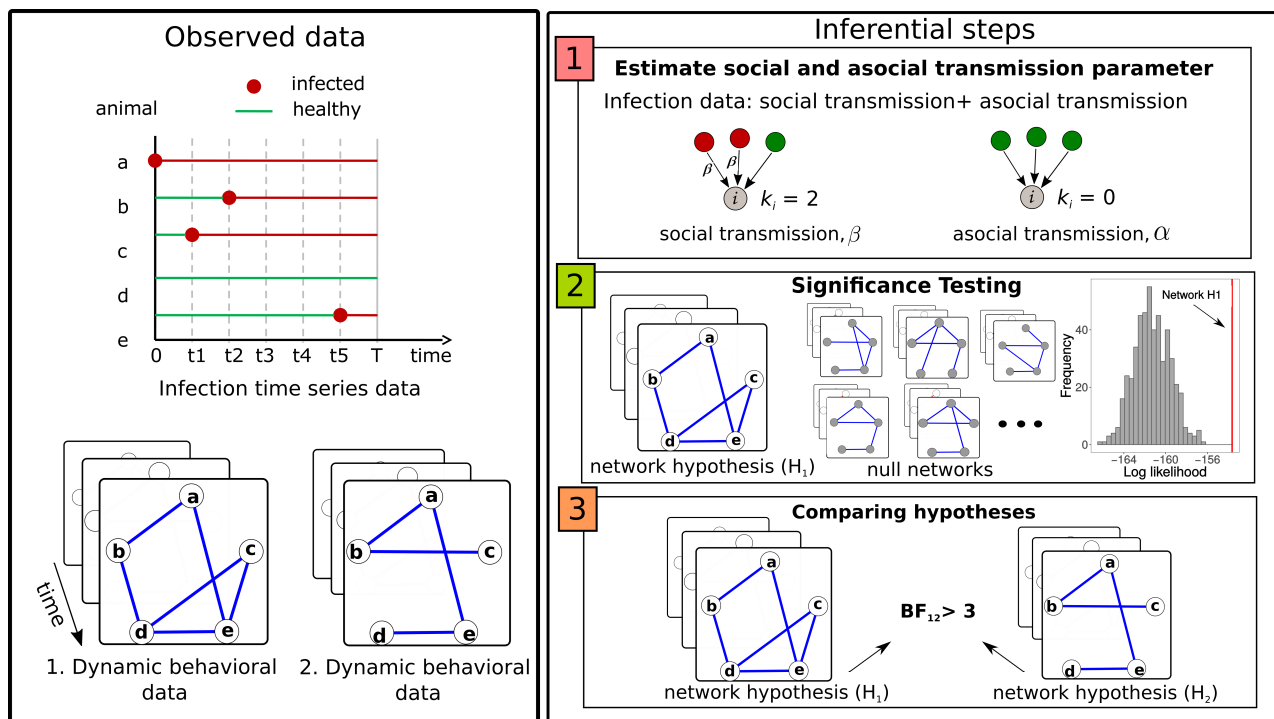


**Figure 1.** Visualization of the steps of our algorithm. **Observed data:** INoDS utilizes the observed infection time-series and dynamic (or static) interaction data to provide evidence towards contact network hypotheses (or hypothesis) using a three step procedure. **Inferential steps:** In the first step, the tool estimates two parameters for a contact network hypothesis - transmission rate  $\beta$ , which represents the component of infection transmission that is contributed by the network connections, and  $\alpha$  that quantifies the component of infection propagation unexplained by the contact network. Significance of  $\beta$  is estimated by comparing the magnitude of social and asocial transmission rate for all observed infection events. Second, the predictive power of the network hypothesis is evaluated by comparing the likelihood of the infection time-series data given the network hypothesis to an ensemble likelihoods derived by permuted null networks. Finally, the marginal likelihood for the given contact network is calculated, which is then used to perform model comparison (using Bayes Factor, BF) in cases where multiple contact network hypotheses are available.

94 the two-fold application of our approach – (i) to identify the specific contact network associated with  
 95 a particular host population, and (ii) to gain epidemiological insights (including the transmission  
 96 mechanism, role of the quality of host contacts) of a host-pathogen system that can be leveraged to  
 97 construct contact networks for predictive modeling of disease spread in host populations at other  
 98 geographical locations.

## 99 Results

100 The primary purpose of INoDS is to obtain evidence towards the contact network that is hypothe-  
 101 sized to be relevant for the spread of an infection through a host population. INoDS also provides  
 102 epidemiological insights of the spreading pathogen by estimating the rate of pathogen transmis-  
 103 sion through the edges of the contact network, and facilitates hypothesis testing on its mode of  
 104 transmission. Evidence is estimated using a three step procedure. First, the tool estimates the  
 105 unknown social ( $\beta$ ) and asocial ( $\alpha$ ) transmission parameter. The social transmission parameter  
 106 quantifies those infection acquisition events that are explained by the edge connections of the  
 107 network hypothesis, while the asocial transmission parameter captures the ‘missingness’ of net-  
 108 work hypothesis in explaining certain infection events. In the second step, the predictive power  
 109 (measured as the likelihood the observed infection time-series data given the network) of network  
 110 hypothesis is compared against a null expectation. The null expectation is generated by permuting  
 111 the edge connections of the dynamic network, while controlling for the number of nodes and  
 112 edges present in the network. A  $P$ -value is estimated as the probability of obtaining the observed

113 predictive power, or something more extreme, if the null expectation were true. In the third step,  
114 marginal (Bayesian) evidence is calculated for the contact network hypotheses; Bayesian evidence  
115 can then be used to perform model selection where more than one contact network hypotheses  
116 exists.

117 In the sections that follow, we evaluate the ac-  
118 curacy of the tool in recovering the transmission  
119 parameters and its ability to identify the under-  
120 lying contact network under common types of  
121 missing data. We further demonstrate the appli-  
122 cation of INoDS by using two empirical dataset: (i)  
123 spread of an intestinal pathogen in bumble bee  
124 colonies, and (ii) salmonella spread in Australian  
125 sleepy lizards.

## 126 INoDS performance

127 We evaluated the performance of INoDS in model  
128 discrimination and recovering the unknown trans-  
129 mission parameters. To do so, we generated hypo-  
130 theoretical infection time-series data by perform-  
131 ing computer simulations of pathogen spread  
132 on a synthetic dynamic network. The synthetic  
133 network was generated by first establishing a  
134 random network (generated by the configuration  
135 model (Molloy and Reed, 1995)) at time-step  $t = 0$ .  
136 For each of the following time stamp, we per-  
137 muted 10% of randomly chosen edges using a  
138 double-edge swap procedure (Molloy and Reed,  
139 1995), for a total of 100 time-steps.

## 140 Accuracy of INoDS in estimating the 141 transmission parameters

142 To test the ability of INoDS to precisely estimate  
143 the social transmission parameter  $\beta$ , we per-  
144 formed 10 independent simulations of SI disease  
145 spread with transmission rates ( $\beta$ ) ranging from  
146 0.01 to 0.1. Model accuracy was determined by  
147 comparing the estimated value of transmission  
148 parameter  $\beta$  to the value of  $\beta$  used to perform  
149 disease simulations. Since the synthetic network  
150 dataset did not contain any missing data, model  
151 accuracy was also tested by evaluating the deviation of the estimated asocial transmission param-  
152 eter  $\alpha$ , from the expected value of zero. In Figure 2, we show that INoDS is able to recover the  
153 true value of  $\beta$  and  $\alpha$ , and that the accuracy of INoDS is independent to the spreading rate of the  
154 pathogen.

## 155 Robustness of INoDS and previous approaches to missing data

156 Model robustness was evaluated against three potential sources of error in data-collection – sam-  
157 pling a subset of individuals in a population (missing nodes), incomplete sampling of interactions  
158 between individuals (missing edges), and infrequent health diagnosis of individuals (missing cases).  
159 Specifically, we randomly removed 10-80% of nodes, edges or infection cases from the simulated  
160 dataset described above. Model robustness was determined as the proportion of times an approach

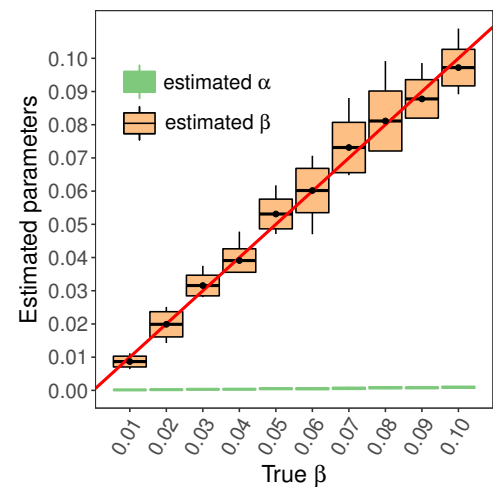


**Figure 2.** INoDS performance on recovering the social ( $\beta$ ) and the asocial ( $\alpha$ ) transmission parameter of simulated susceptible-infected (SI) model of infectious disease spread. Disease simulations were performed on dynamic networks with 100 nodes, Poisson degree distribution, mean degree of 4, and 100 discrete time snapshots. Each boxplot summarizes the results of 10 independent disease simulations; the horizontal line in the middle is the mean of estimated parameter values, the top and the bottom horizontal line is the standard deviation, and the tip of the vertical line represents the maximum/minimum value. The solid red line represents one-to-one correspondence between the  $\beta$  value estimated by INoDS and the value of  $\beta$  used for disease simulations. Since the simulations were performed on a known synthetic network, the expected value of asocial transmission parameter is zero.

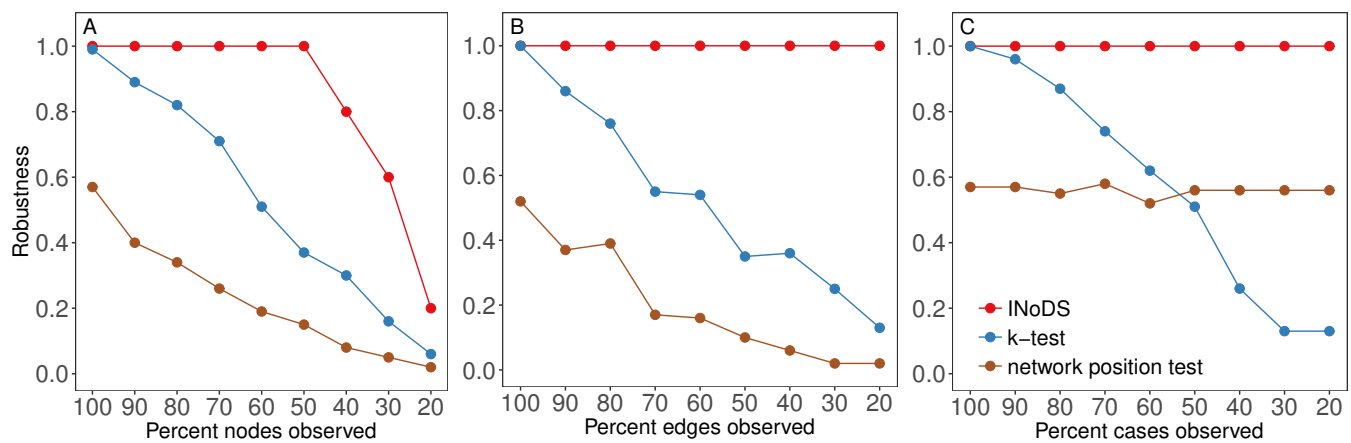


**Figure 3.** Robustness of INoDS,  $k$ -test and network position test to three common forms of missing data - missing nodes, missing edges and missing infection cases. Robustness is calculated as 1 - false negative rate of the test. To calculate the false negative rate, null expectation in INoDS and network position test is generated by permuting the edge connections of the observed networks, creating an ensemble of null networks. On the other hand, in  $k$ -test the location of infection cases within the observed network are permuted, creating a permuted distribution of  $k$ -statistic.

161 correctly assigned the observed network with a high statistical power ( $P < 0.05$ ). We compared  
 162 the robustness of INoDS to two previous approaches –  $k$ -test procedure and network position  
 163 test. The  $k$ -test procedure involves estimating the mean infected degree (i.e., number of direct  
 164 infected contacts) of each infected individual in the network, called the  $k$ -statistic. The  $P$ -value in  
 165  $k$ -test is calculated by comparing the observed  $k$ -statistic to a distributed of null  $k$ -statistics which  
 166 is generated by randomizing the node-labels of infection cases in the network (*VanderWaal et al.,*  
 167 **2016**). Network position test compares the degree of infected individuals to that of uninfected indi-  
 168 viduals. The observed network is considered to be epidemiologically relevant when the difference  
 169 in average degree between infected and uninfected individuals exceeds (at 5% significance level)  
 170 the degree difference in an ensemble of permuted networks. Figure 3 summarizes the results.  
 171 INoDS correctly assigns the observed network with a higher statistical power across a wide range of  
 172 incomplete sampling scenarios. The tool is least sensitive to missing edges in the observed network  
 173 and unobserved infection cases. For data with incomplete sampling of nodes, the statistical power  
 174 of INoDS remains close to one when at least 50% of nodes were observed in the network. We  
 175 also find that the robustness of this approach is relatively unaffected by the edge density of the  
 176 underlying contact network (Appendix Fig 1). On the other hand,  $k$ -test and network position test  
 177 were sensitive to all types of missing data. Robustness of  $k$ -test procedure rapidly declined with  
 178 any increase in missing data on the nodes, edges of the observed contact network, and infected  
 179 cases. Out of the three approaches, network position test proved to be the least reliable as its false  
 180 negative rate was high even when no data were missing.

### 181 Applications to empirical data-sets

182 We demonstrate the application of INoDS to perform hypothesis testing on contact networks of  
 183 infectious disease spread, identify transmission mechanisms and infer transmission rate using two  
 184 real-world datasets. The first dataset is derived from the study by *Otterstatter and Thomson (2007)*  
 185 that examined the spread of an intestinal pathogen (*Crithidia bombi*) within the colonies of social  
 186 bumble bee *Bombus impatiens*. The second dataset examines the spread of *Salmonella enterica*  
 187 within two wild populations of Australian sleepy lizards *Tiliqua rugosa* (*Bull et al., 2012*).

### 188 Determining the role of edge weights in contact network model: case study of the 189 spread of *Crithidia bombi* in bumble bee colonies

190 The data consists of dynamic networks of bee colonies ( $N = 5-7$  individuals), where edges represent  
 191 direct physical contacts that were recorded using a color-based video tracking software. A bumble

192 bee colony consists of a single queen bee and infertile foragers. Infection experiments were  
193 performed on seven colonies; in five colonies infection was introduced by their naturally infected  
194 queens, while in the remaining two colonies one forager was randomly selected to be artificially  
195 infected. Infection progression through the colonies was tracked by regularly screening the faeces  
196 of each bee in the colony, and the infection timing was determined using the knowledge of the  
197 rate of replication of *C. bombi* within its host intestine. *Otterstatter and Thomson (2007)* showed  
198 that the infection timings of susceptible bees in the colony was associated with their frequency  
199 of contacts with infected nest-mates rather than the duration of contacts. Here, we extend the  
200 results of the previous study by addressing two specific questions: (1) Do networks where edges  
201 represent physical contact have a high predictive power to predict the spread of *C. bombi* than  
202 random networks? (2) Should the edges in contact network be weighted (by frequency or duration)  
203 of contacts, or unweighted?

204 The contact networks collected in the previous study were fully connected. As fully connected  
205 network rarely describe the dynamics of infection spread, we created sparser contact networks  
206 by sequentially removing a certain percentage of weak weighted edges. Specifically, edges with  
207 weights less than 10-50% of the highest edge-weight were removed to generate contact network  
208 hypotheses with a range of edge-densities. In addition, four types of contact networks with different  
209 edge-weights were constructed - networks where edges were weighted with respect to frequency of  
210 contacts, edge weighted by duration of contacts, and edges with no edge weights (i.e., binary edges).  
211 Since the technique of creating sparser networks involved removal of weak weighted edges, two  
212 types of binary contact networks were constructed - binary networks whose edge connections were  
213 the same as frequency weighted contact networks, and binary networks whose edge connections  
214 were similar to duration weighted contact networks.

215 Figure 4 A-D shows the parameter estimates for the four types of contact network hypotheses at  
216 different edge weight thresholds. Generally, the rate of infection transfer through social connections  
217 was higher than asocial transmission for contact networks where less than 20% of weakest edge  
218 weights were removed (dark blue bars in Figure 4). In addition, frequency weighted contact networks  
219 (with 5-10% of weakest edge weights removed) were associated with highest Bayesian evidence in  
220 all of the analyzed bee colonies (Figure 4E, Appendix figure 3).

## 221 **Identifying contact network model using imperfect disease data: case study of** 222 ***Salmonella enterica* spread in Australian sleepy lizard populations**

223 This dataset monitors the spread of the commensal bacterium *Salmonella enterica* in two separate  
224 wild populations of Australian sleepy lizard *Tiliqua rugosa* (*Bull et al., 2012*). The two sites consisted  
225 of 43 and 44 individuals respectively, and these represented close to 100% of all adult lizards at the  
226 two sites (i.e., no other individuals were encountered during the study period). Individuals were  
227 fitted with GPS loggers and their locations were recorded every 10 minutes for 70 days. Following  
228 *Bull et al. (2012)*, we constructed proximity networks by assuming a contact between individuals  
229 whenever the location of two lizards was recorded to be within 14m distance of each other. The  
230 dynamic networks at both sites consisted of 70 static snapshots, with each snapshot summarizing a  
231 day of interactions between the lizards. *Salmonella* infection were monitored at the two populations  
232 using single cloacal swabs on each animal once every 14 days. Consequently, the disease data  
233 in this system represents the timing of *diagnoses* instead of actual infection timings of lizards in  
234 the two populations. Since lizards are known to recover from *Salmonella* infection, and eventually  
235 get reinfected, we assumed the infection to follow a SIS (susceptive-infected-susceptible) disease  
236 model.

237 To test the hypothesis that the proximity interactions of sleepy lizards are predictive of *Salmonella*  
238 spread, we formed two hypothesis of contact network models - i) proximity networks with binary  
239 edges, and ii) proximity networks where edges were weighted by frequency (i.e., the total number)  
240 of interactions between individuals. Employing Bayesian data augmentation method, we considered  
241 the actual infection timings to be unobserved parameters, which was sampled for each contact

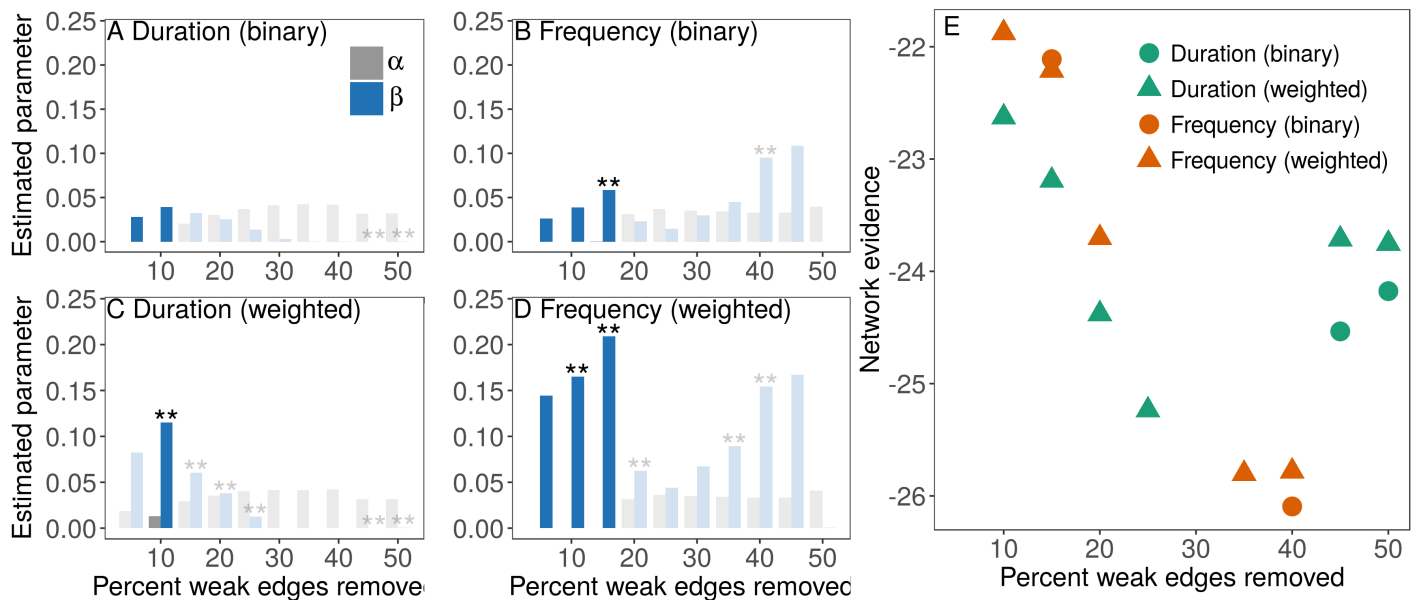


**Figure 4.** Identifying the contact network of *Crithidia* spread in bumble bee colony (colony UN2). (A-D) Edges in the contact network models represent physical interaction between the bees. Since the networks were fully connected, a series of filtered contact networks were constructed by removing weak weighted edges in the network. The x-axis represents the edge-weight threshold that was used to removed weak edges in the network. Two types of edge weights were tested - frequency and duration of contacts. In addition, across all ranges of percent weak edges removed, the two types of weighted network were converted to binary networks. The results shown are estimated values of social transmission parameter  $\beta$ , and estimated values of asocial transmission parameter  $\alpha$ , for the different contact network hypotheses. Asterisks (\*\*) indicate significant predictive power of the contact network hypothesis as compared to an ensemble of permuted networks. The darker blue color corresponds to the networks, where the social transmission rate was significantly higher than the asocial transmission. (E) Log Bayesian (marginal) evidence of the contact networks with high predictive power (i.e., networks marked with asterisks in A-D)

242 network hypothesis (along with transmission parameters) using data on diagnosis timings. Figure  
 243 5 summarizes the results of significance testing (step 2 of INoDS analysis) for site 1. We found  
 244 that the likelihood of Salmonella infection spreading through the weighted proximity network was  
 245 significantly greater than the null expectation (Figure 5b). In contrast, the predictive power of binary  
 246 proximity network was statistically insignificant ( $P = 0.602$ ). Bayes factor of the weighted network  
 247 versus the binary network was 817.09 which indicates that the occurrence of repeated contacts  
 248 between two individuals, rather than just the presence of a contact, is important for Salmonella  
 249 transmission. Analysis of the two network hypotheses at the second site yielded similar results,  
 250 although the binary network at the site was also found to be statistically significant (albeit with low  
 251 predictive power as compared to the weighted network, Appendix 1 Figure 1).

## 252 Discussion

253 Network modeling of infectious disease spread is becoming an increasingly popular approach, as  
 254 the quality of data that can be collected from animal populations has dramatically improved in  
 255 recent years owing to the use of modern technology. However, the concepts of power analysis and  
 256 hypothesis testing are still underdeveloped in network modeling, even though such approaches are  
 257 widely recognized as key elements to establish the level of 'informativeness' and appropriateness of  
 258 a model (Jennions and Møller, 2003; Johnson et al., 2015). Our ability to define a contact network  
 259 relies on our knowledge about the host behavior, and the dominant mode of transmission of the  
 260 pathogen. Since such knowledge is either derived from expert knowledge (which can be subjective)  
 261 or laboratory experiments (which are time- and resource-intensive), it is essential to conduct an a  
 262 priori analysis of contact network models to avoid uninformative or misleading disease predictions.

263 In this study we therefore present INoDS as a tool that performs network model selection and  
 264 establishes the predictive power of a contact network model to describe the observed infection

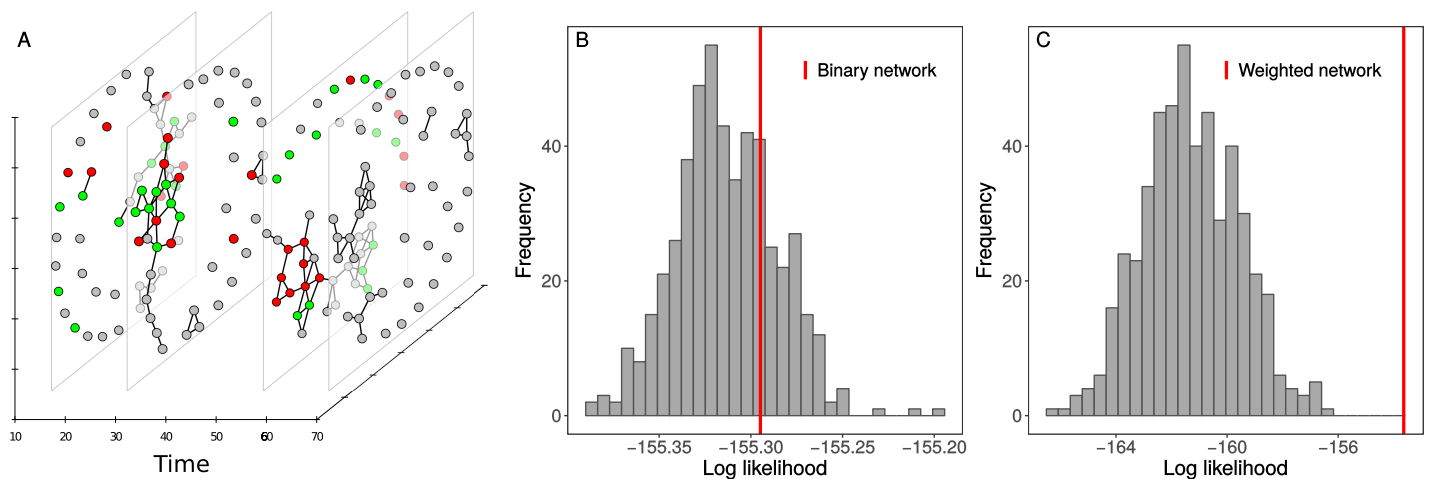


**Figure 5.** Identifying the contact network of *Salmonella* spread in Australian sleepy lizards. (A) Dynamic network of proximity interactions between 43 lizards in a population recorded for a total duration of 70 days. Each temporal slice summarizes interaction within a day. Node colors denote the infection status confirmed by laboratory diagnosis. Green nodes are the animals that were diagnosed to be not infected at that time-point, red are the animals that were diagnosis to be infected and grey nodes are the individuals with unknown infection status at time-point. We hypothesized that proximity network with edges that were either binary or weighted with respect to the frequency of interactions could potentially explain the observed spread of *Salmonella* in the population. We found that (B) the predictive power of binary networks was statistically insignificant ( $P = 0.602$ , log-Bayesian evidence =  $-1039.89$ ), whereas (C) proximity networks with frequency weighted edges demonstrated a significantly greater predictive power than a random expectation ( $P < 0.001$ , log-Bayesian evidence =  $-222.80$ ). The log Bayes factor of the weighted contact network versus binary contact network, is 817.09, which is a decisive evidence towards the frequency weighted proximity network model.

265 spread. INoDS also provides epidemiological insights about the spreading pathogen by enabling  
266 hypothesis testing on different transmission mechanisms, and estimating the rate of pathogen  
267 transmission through contacts between individuals (social transmission parameter,  $\beta$ ). Unlike  
268 previous approaches, INoDS is robust to missing network data, imperfect disease surveillance,  
269 and can provide network inference for a range of disease spread models. The tool can thus be  
270 used to provide inference on contact networks for a variety of infection spread occurring both  
271 in human and non-human species. Inferring the role of dynamic contacts on infectious disease  
272 spread requires the knowledge of either order or timing of infection of individuals in the network. In  
273 practice, constraints on data collection (for e.g., due to infrequent health assessments), or infection  
274 diagnostics (for e.g., due to sub-clinical infection, poor diagnostics) precludes the knowledge of  
275 precise timing of infection acquisition in a host population. To overcome this challenge, our tools  
276 assumes the infection timings in a host population to be unobserved, and uses data on infection  
277 diagnosis instead to provide inference on contact networks.

278 As such, our approach addresses a growing subfield in network epidemiological theory that uses  
279 statistical tools to infer contact network models using all available host and disease data (Welch  
280 et al., 2011; Stack et al., 2013). The proposed tool in this study can be used to tackle several funda-  
281 mental challenges in the field of infectious disease modeling (Eames et al., 2015). First, INoDS can  
282 be used to perform model selection on contact network models that quantify different transmission  
283 modes; this approach therefore facilitates the identification of infection-transmitting contacts and  
284 does not rely on laboratory experimentation (or subjective expert knowledge). Second, INoDS can  
285 be used to establish the predictive power of proxy measures of contact in cases where limited  
286 interaction data is example. For example, spatial proximity, home-range overlap or asynchronous  
287 refuge use are commonly used as a proxy of contact in wild animal populations (Godfrey et al.,  
288 2010; Leu et al., 2010; Sah et al., 2016). INoDS establishes the epidemiological significance of such  
289 assumptions by comparing the likelihood of infection spread occurring along the edges of the proxy  
290 contact network to the likelihoods generated from an ensemble of random networks. Third, it is  
291 well known that not all contacts between the hosts have the same potential for infection transfer.

292 The heterogeneity of host contacts in a network model is typically captured through edge weights,  
293 but it often not clear which type of edge weights (frequency, duration or intensity) is relevant in the  
294 context of a specific host pathogen system (Pellis *et al.*, 2014). Through model selection of contact  
295 networks with similar edge connects but different edge weight criterion, INoDS can help establish a  
296 link between edge weight and the risk of transmission across an edge in the contact network.

297 We demonstrate the application of INoDS using two real world datasets. In the first dataset, we  
298 used INoDS to determine the role of edge weight and edge weight type on the predictive power  
299 of the contact network. To accurately model the spread of *Crithidia* gut protozoan in bumble bee  
300 colonies, we show that the contact networks should be weighted with respect to frequency, rather  
301 than the duration, of contacts between individual. Our results therefore support the original finding  
302 of the study (Otterstatter and Thomson, 2007), where individual's risk of infection was found to be  
303 correlated with their contact rate with infected nest-mates. However, our results show that edges  
304 below a certain edge weight threshold do not play an important role in infection transfer. Contact  
305 networks where such weak weighted edges have been removed, therefore, demonstrate higher  
306 predictive power than fully connected networks. In the next empirical example, we explore two  
307 transmission mechanisms of a commensal bacterium in wild population of Australian sleepy lizards  
308 - direct transfer of bacterium through host physical proximity and indirected transfer measured by  
309 the extent of host's home-range overlap. Our results show that contact networks of host's spatial  
310 proximity predict the infection spread in lizard population rather than contact network based on  
311 home-range overlap. These findings support a previous study which suggests that the bacterial  
312 transmission could occur between closely located animals through contaminated faecal scats rather  
313 than indirect environmental transmission (Bull *et al.*, 2012).

314 The current version of INoDS, assumes the infection has no latent period, and that the infectious-  
315 ness of infected hosts and susceptibility of naive hosts is equal for all individuals in the population.  
316 In future, these assumptions can be easily relaxed to incorporate more complex formulations  
317 of pathogen spread through a host population. For instance, heterogeneity in infectiousness of  
318 infected hosts and susceptibility of naive hosts can be incorporated as random effects in the model  
319 by assuming the two to follow a Gaussian distribution. Disease latency can be incorporated using  
320 the data-augmentation technique described in the paper.

321 To summarize, we have designed a simple and general framework that provides inference  
322 on contact network underling infectious disease spread, given the host behavior and infection  
323 incidence data. Our approach is robust to missing data, and does not require information on the  
324 actual infection timings in the population, which is rarely available. The tool described in the this  
325 study, on one hand, can be used to establish the power of a contact network model to make reliable  
326 disease predictions; on the other hand, the tool can be used to gain epidemiological insights (such  
327 as the mode of infection transfer, role of quality of host contacts) for host-pathogen systems. Since  
328 data-collection for network analysis can be labor-intensive and time-consuming, so it is essential to  
329 make decisions on how limited data collection resources are deployed. Based on the sensitivity  
330 analysis of our tool to missing data, we learn that the data-collection efforts should aim to sample  
331 as many individuals in the population as possible, since missing nodes have the greatest impact  
332 (rather than missing edges) on the predictive power of network models. In future, INoDS can be  
333 used to improve targeted disease management and control by identifying high-risk behaviors and  
334 super-spreaders of a novel pathogen without relying on expensive transmission experiments that  
335 take years to resolve.

## 336 **Methods**

337 Here we describe INoDS, a computational tool for identifying underlying contact networks of  
338 infectious disease spread. INoDS provides evidence towards a contact network model, and enables  
339 discrimination of competing contact network hypotheses, including those based on pathogen  
340 transmission mode, edge weight criteria and data collection techniques. In order to run INoDS,  
341 the following two types of data are required as an input: infection time series data, which includes

342 infection diagnoses (coded as 0 = not infected and 1 = infected), and timestep of diagnosis for all  
343 available nodes in the networks; and edge-list of dynamic (or static) contact network. An edge-list  
344 format is simply the list of node pairs (each node pair represents an edge of the network), along  
345 with the weight assigned to the edge and time-step of interaction, with one node pair per line. The  
346 software is implemented in Python, is platform independent, and is freely available at ([link - to be  
347 updated](#)).

### 348 **INoDS formulation**

349 We assume that at each instance the infection potential for an individual  $i$  depends on two process -  
350 (a) social transmission  $\beta$ , that is captured by the edge connections in the contact network hypothesis,  
351 and (b) asocial transmission  $\alpha$ , that represents those infection events that are not explained by the  
352 edge connections. The infection potential,  $\lambda_i(t_i)$ , of individual  $i$  at the time of acquisition of infection  
353  $t_i$  is then calculated as:

$$\lambda_i(t_i) = 1 - \exp\{-\beta k_i(t_i - 1) - \alpha\} \quad (1)$$

354 where  $k_i(t - 1)$  denotes the number of infected connections of the focal individual  $i$  at the  
355 previous time-step  $(t - 1)$  as determined by the network hypothesis.

356 The log-likelihood for all observed timing of infection in a population given the network hypoth-  
357 esis ( $H_A$ ) can therefore be estimated as:

$$\log(D|H_A, \beta, \alpha) = \sum^n \log[\lambda_n(t_n)] + \sum^t \left( \sum^m \log[1 - \lambda_m(t)] \right) \quad (2)$$

358 where  $t_n$  is the time of infection of individual  $n$ . The first part of equation 2 therefore estimates  
359 the log likelihood of all observed infection acquisition events. The second part of the equation  
360 represents the log-likelihood of susceptible individuals  $m$  remaining uninfected at time  $t$ .

### 361 **Data augmentation for unknown infection and recovery time**

362 Calculation of network likelihood using equation 2 requires the knowledge of exact timing of  
363 infection,  $t_1, \dots, t_n$ , for  $n$  infected individuals in the population. However in many cases, the only  
364 data that is available are the timings of when individuals in a populations were *diagnosed* to be  
365 infected,  $d_1, \dots, d_n$ . We therefore employ a Bayesian data augmentation approach to estimate the  
366 actual infection timings in the disease dataset *Tanner and Wong (1987)*. Since the actual infection  
367 time  $t_i$  for an individual  $i$  is unobserved, we only know that the time of infection for individual  
368  $i$  lies between the interval  $(L_i, d_i]$ , where  $L_i$  is the last negative diagnosis of individual  $i$  before  
369 infection acquisition. Within this interval, the individual could have potentially acquired infection  
370 at any time-step where it was in contact with other infected individuals in the network. Assuming  
371 incubation period to be one time-step, we can therefore represent the potential set of infection  
372 time as  $t_i \in \{g_i(t - 1) > 0, L_i < t_i \leq d_i\}$ , where  $g_i(t - 1)$  is the degree (number of contacts) of individual  
373  $i$  at time  $t - 1$ . The data augmentation proceeds in two steps. In the first step, the missing infection  
374 times are imputed conditional on the possible set of infection times. In the next step the posterior  
375 distributions of the unknown parameters are sampled based on the imputed data. We performed  
376 data imputation using inverse transform sampling method, which is a technique of drawing random  
377 samples from any probability distribution given its cumulative distribution function (*Robert and  
378 Casella, 2004*). For infections that follow a SIS or SIR disease model, it is essential to impute the  
379 recovery time of infected individuals for accurate estimation of infected degree. To do so, we adopt  
380 a similar data augmentation approach as described before. We performed data imputation by  
381 drawing random samples from the set of possible recovery time-points using the inverse transform  
382 sampling technique.

### 383 **Estimating the transmission parameters**

384 We adopt a Bayesian approach to estimate the social  $\beta$  and asocial  $\alpha$  transmission parameters.  
385 We use Markov chain Monte Carlo (MCMC) technique with flat priors to obtain, after a burn-in  
386 period, the joint posterior density for the parameters. Using Bayes' Theorem, the joint posterior  
387 distribution of for a set  $\Theta$  of parameters can be written as

$$P(\Theta|D, H) = \frac{\mathcal{L}(D|H, \Theta)\mathcal{P}(\Theta|H)}{\mathcal{E}(D|H)} \propto \mathcal{L}(D|H, \Theta)\mathcal{P}(\Theta|H) \quad (3)$$

388 where  $D$  is the infection time-series data,  $H$  is the contact network hypothesis, and  $P, \mathcal{L}, \mathcal{P}, \mathcal{E}$   
389 are the shorthands for the posterior, the likelihood, the prior and the evidence, respectively. To  
390 obtain the posterior distributions, we use *emcee* package in Python (*Foreman-Mackey et al., 2013*).

### 391 **Testing the significance of social transmission parameter**

392 To test for the significance of the social transmission parameter ( $\beta$ ), the social transmission rate is  
393 compared to the asocial transmission rate for each infected individual. The estimated value of  $\beta$  is  
394 considered to be statistically significant when the asocial component of infection potential ( $=\alpha$ ) is  
395 greater than the social component ( $=\beta k_i(t_i - 1)$ ) in fewer than 5% of the infection cases.

### 396 **Testing the predictive power of a contact network hypothesis**

397 To assess the significance of the contact network hypothesis, we compare the likelihood of the  
398 infection time-series data given the contact network and estimated transmission parameter (i.e.,  
399  $\mathcal{L}(D|H, \Theta)$ ) to a distribution of likelihoods of infection data for randomized networks. Randomized  
400 networks are generated by randomizing edge connections in the contact network hypothesis, which  
401 preserves the edge-density in the permuted networks. A  $p$ -value is calculated as the proportion of  
402 randomizations which generate a likelihood more extreme than the likelihood under the network  
403 hypothesis. A contact network with a  $p$ -value of less than 0.05 is considered to demonstrate a  
404 substantive greater predictive power than the null expectation.

### 405 **Performing model selection of competing network hypotheses**

406 To facilitate model selection in cases where there are more than one network hypothesis, we  
407 compute marginal likelihood of the infection data given each contact network model. The marginal  
408 likelihood, also called the Bayesian evidence, measures the overall model fit, i.e., to what extent  
409 the infection time-series data can be simulated by a network hypothesis ( $H_1$ ). Bayesian evidence  
410 is based on the average model fit, and calculated by integrating the model fit over the entire  
411 parameter space:

$$P(D|H, \Theta) = \int \mathcal{P}(\Theta|H)\mathcal{L}(D|H, \Theta)d\Theta \quad (4)$$

412 Since it is difficult to integrate Eq.4 numerically, we estimate the marginal likelihood of network  
413 models using thermodynamic integration, or path sampling (*Lartillot and Philippe, 2006*) method  
414 implemented in *emcee* package in Python.

415 Model selection can be then performed by computing pair-wise Bayes factor, i.e. the ratio of the  
416 marginal likelihoods of two network hypotheses. The log Bayes' factor to assess the performance  
417 of model  $M_1$  over model  $M_2$ , is expressed as:

$$\log(B_{21}) = \log(P(D|H_2)) - \log(P(D|H_1)) \quad (5)$$

418 The contact network with a higher marginal likelihood is considered to be more plausible, and  
419 a log Bayes' factor of more than 3 is considered to be a strong support in favor of the alternative  
420 network model ( $H_2$ ) (*Kass and Raftery, 1995*).

## 421 Acknowledgments

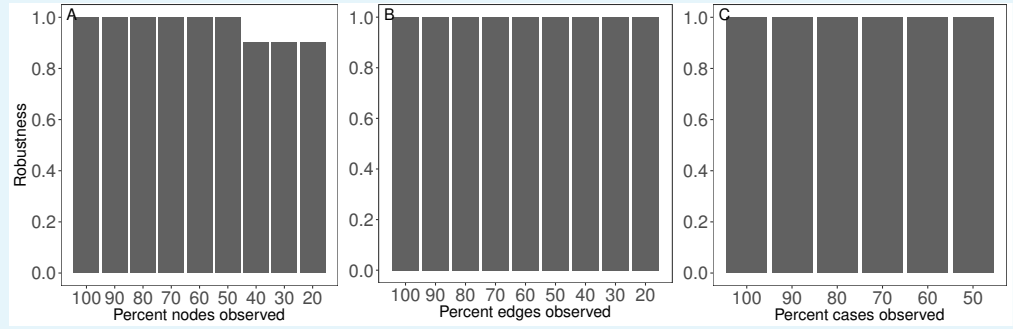
422 This work was supported by the National Science Foundation Ecology and Evolution of Infectious  
423 Diseases Grant 1216054.

## 424 References

- 425 **Aiello CM**, Nussear KE, Esque TC, Emblidge PG, Sah P, Bansal S, et al. Host contact and shedding patterns clarify  
426 variation in pathogen exposure and transmission in threatened tortoise *Gopherus agassizii*: implications  
427 for disease modeling and management. *Journal of Animal Ecology*. 2016; p. n/a–n/a. doi: [10.1111/1365-  
428 2656.12511](https://doi.org/10.1111/1365-2656.12511).
- 429 **Bansal S**, Grenfell BT, Meyers LA. When individual behaviour matters: homogeneous and network models  
430 in epidemiology. *Journal of the Royal Society, Interface / the Royal Society*. 2007 oct; 4(16):879–91. doi:  
431 [10.1098/rsif.2007.1100](https://doi.org/10.1098/rsif.2007.1100).
- 432 **Bansal S**, Read J, Pourbohloul B, Meyers LA. The dynamic nature of contact networks in infectious disease  
433 epidemiology. *Journal of Biological Dynamics*. 2010; 4(5):478–489. doi: [10.1080/17513758.2010.503376](https://doi.org/10.1080/17513758.2010.503376).
- 434 **Bull CM**, Godfrey SS, Gordon DM. Social networks and the spread of Salmonella in a sleepy lizard population.  
435 *Molecular Ecology*. 2012; 21(17):4386–4392. doi: [10.1111/j.1365-294X.2012.05653.x](https://doi.org/10.1111/j.1365-294X.2012.05653.x).
- 436 **Craft ME**, Caillaud D. Network models: An underutilized tool in wildlife epidemiology? *Interdisciplinary  
437 Perspectives on Infectious Diseases*. 2011 jan; 2011:676949. doi: [10.1155/2011/676949](https://doi.org/10.1155/2011/676949).
- 438 **Danon L**, Ford AP, House T, Jewell CP, Keeling MJ, Roberts GO, et al. Networks and the epidemiology of  
439 infectious disease. *Interdisciplinary perspectives on infectious diseases*. 2011 jan; 2011:284909. doi:  
440 [10.1155/2011/284909](https://doi.org/10.1155/2011/284909).
- 441 **Eames K**, Bansal S, Frost S, Riley S. Six challenges in measuring contact networks for use in modelling. *Epidemics*.  
442 2015; 10:72–77. doi: [10.1016/j.epidem.2014.08.006](https://doi.org/10.1016/j.epidem.2014.08.006).
- 443 **Farine D**. The dynamics of transmission and the dynamics of networks. *Journal of Animal Ecology*. 2017;  
444 86(3):415–418. doi: [10.1111/1365-2656.12659](https://doi.org/10.1111/1365-2656.12659).
- 445 **Fefferman NH**, Ng KL. How disease models in static networks can fail to approximate disease in dynamic net-  
446 works. *Physical Review E - Statistical, Nonlinear, and Soft Matter Physics*. 2007; 76(3):1–11. doi: [10.1103/Phys-  
447 RevE.76.031919](https://doi.org/10.1103/PhysRevE.76.031919).
- 448 **Fenner AL**, Godfrey SS, Michael Bull C. Using social networks to deduce whether residents or dispersers  
449 spread parasites in a lizard population. *Journal of Animal Ecology*. 2011; 80(4):835–843. doi: [10.1111/j.1365-  
450 2656.2011.01825.x](https://doi.org/10.1111/j.1365-2656.2011.01825.x).
- 451 **Foreman-Mackey D**, Hogg DW, Lang D, Goodman J. emcee: The MCMC Hammer. *Publications of the Astronom-  
452 ical Society of the Pacific*. 2013; 125(925):306–312. doi: [10.1086/670067](https://doi.org/10.1086/670067).
- 453 **Godfrey SS**. Networks and the ecology of parasite transmission: A framework for wildlife parasitol-  
454 ogy. *International journal for parasitology Parasites and wildlife*. 2013 dec; 2(1):235–245. doi:  
455 [10.1016/j.ijppaw.2013.09.001](https://doi.org/10.1016/j.ijppaw.2013.09.001).
- 456 **Godfrey SS**, Bull CM, James R, Murray K. Network structure and parasite transmission in a group living  
457 lizard, the gidgee skink, *Egernia stokesii*. *Behavioral Ecology and Sociobiology*. 2009; 63(7):1045–1056. doi:  
458 [10.1007/s00265-009-0730-9](https://doi.org/10.1007/s00265-009-0730-9).
- 459 **Godfrey SS**, Moore JA, Nelson NJ, Bull CM. Social network structure and parasite infection patterns in a territorial  
460 reptile, the tuatara (*Sphenodon punctatus*). *International Journal for Parasitology*. 2010; 40(13):1575–1585.  
461 doi: [10.1016/j.ijpara.2010.06.002](https://doi.org/10.1016/j.ijpara.2010.06.002).
- 462 **Hamede RK**, Bashford J, McCallum H, Jones M. Contact networks in a wild Tasmanian devil (*Sarcophilus  
463 harrisii*) population: using social network analysis to reveal seasonal variability in social behaviour and its  
464 implications for transmission of devil facial tumour disease. *Ecology letters*. 2009 nov; 12(11):1147–57. doi:  
465 [10.1111/j.1461-0248.2009.01370.x](https://doi.org/10.1111/j.1461-0248.2009.01370.x).
- 466 **Jennions M**, Møller A. A survey of the statistical power of research in behavioral ecology and animal behavior.  
467 *Behavioral Ecology*. 2003; 14(3):438–445. doi: [10.1093/beheco/14.3.438](https://doi.org/10.1093/beheco/14.3.438).

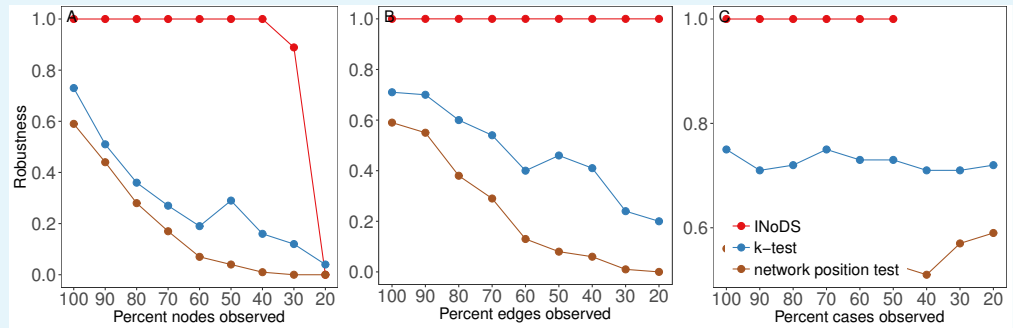
- 468 **Johnson PCD**, Barry SJE, Ferguson HM, Müller P. Power analysis for generalized linear mixed models in ecology  
469 and evolution. *Methods in Ecology and Evolution*. 2015; 6(2):133–142. doi: [10.1111/2041-210X.12306](https://doi.org/10.1111/2041-210X.12306).
- 470 **Kass R**, Raftery A. Bayes Factors. *Journal of the American Statistical Association*. 1995; 90(430):773–795. doi:  
471 [10.1080/01621459.1995.10476572](https://doi.org/10.1080/01621459.1995.10476572).
- 472 **Lartillot N**, Philippe H. Computing Bayes Factors Using Thermodynamic Integration. *Systematic Biology*. 2006;  
473 55(2):195–207. doi: [10.1080/10635150500433722](https://doi.org/10.1080/10635150500433722).
- 474 **Leu ST**, Kappeler PM, Bull CM. Refuge sharing network predicts ectoparasite load in a lizard. *Behavioral ecology*  
475 and sociobiology. 2010 sep; 64(9):1495–1503. doi: [10.1007/s00265-010-0964-6](https://doi.org/10.1007/s00265-010-0964-6).
- 476 **MacIntosh AJJ**, Jacobs A, Garcia C, Shimizu K, Mouri K, Huffman Ma, et al. Monkeys in the middle: para-  
477 site transmission through the social network of a wild primate. *PloS one*. 2012 jan; 7(12):e51144. doi:  
478 [10.1371/journal.pone.0051144](https://doi.org/10.1371/journal.pone.0051144).
- 479 **Molloy M**, Reed B. A Critical Point for Random Graphs With a Given Degree Sequence. *Random Structures and*  
480 *Algorithms*. 1995; 6(2-3):161–180.
- 481 **Otterstatter MC**, Thomson JD. Contact networks and transmission of an intestinal pathogen in bumble bee  
482 (*Bombus impatiens*) colonies. *Oecologia*. 2007 nov; 154(2):411–21. doi: [10.1007/s00442-007-0834-8](https://doi.org/10.1007/s00442-007-0834-8).
- 483 **Pellis L**, Ball F, Bansal S, Eames K, House T, Isham V, et al. Eight challenges for network epidemic models.  
484 *Epidemics*. 2014; 10:58–62. doi: [10.1016/j.epidem.2014.07.003](https://doi.org/10.1016/j.epidem.2014.07.003).
- 485 **Robert C**, Casella G. Monte Carlo Statistical Methods. Springer Texts in Statistics; 2004.
- 486 **Sah P**, Leu ST, Cross PC, Hudson PJ, Bansal S. Unraveling the disease consequences and mechanisms of modular  
487 structure in animal social networks. *Proceedings of the National Academy of Sciences of the United States of*  
488 *America*. 2017 apr; 114(16):4165–4170. doi: [10.1073/pnas.1613616114](https://doi.org/10.1073/pnas.1613616114).
- 489 **Sah P**, Nussear KE, Esque TC, Aiello CM, Hudson PJ, Bansal S. Inferring social structure and its drivers from  
490 refuge use in the desert tortoise, a relatively solitary species. *Behavioral Ecology and Sociobiology*. 2016; p.  
491 1–13. doi: [10.1007/s00265-016-2136-9](https://doi.org/10.1007/s00265-016-2136-9).
- 492 **Stack JC**, Bansal S, Anil Kumar VS, Grenfell B. Inferring population-level contact heterogeneity from common  
493 epidemic data. *Journal of the Royal Society, Interface / the Royal Society*. 2013; 10(78):20120578. doi:  
494 [10.1098/rsif.2012.0578](https://doi.org/10.1098/rsif.2012.0578).
- 495 **Tanner MA**, Wong WH. The Calculation of Posterior Distributions by Data Augmentation: Rejoinder. *Journal of*  
496 *the American Statistical Association*. 1987; 82(398):548–550. doi: [10.2307/2289463](https://doi.org/10.2307/2289463).
- 497 **VanderWaal K**, Enns EA, Picasso C, Packer C, Craft ME. Evaluating empirical contact networks as potential  
498 transmission pathways for infectious diseases. *Journal of The Royal Society Interface*. 2016; 13(121):20160166.  
499 doi: [10.1098/rsif.2016.0166](https://doi.org/10.1098/rsif.2016.0166).
- 500 **Welch D**, Bansal S, Hunter DR. Statistical inference to advance network models in epidemiology. *Epidemics*.  
501 2011; 3(1):38–45. doi: [10.1016/j.epidem.2011.01.002](https://doi.org/10.1016/j.epidem.2011.01.002).

502 **Appendix 1**



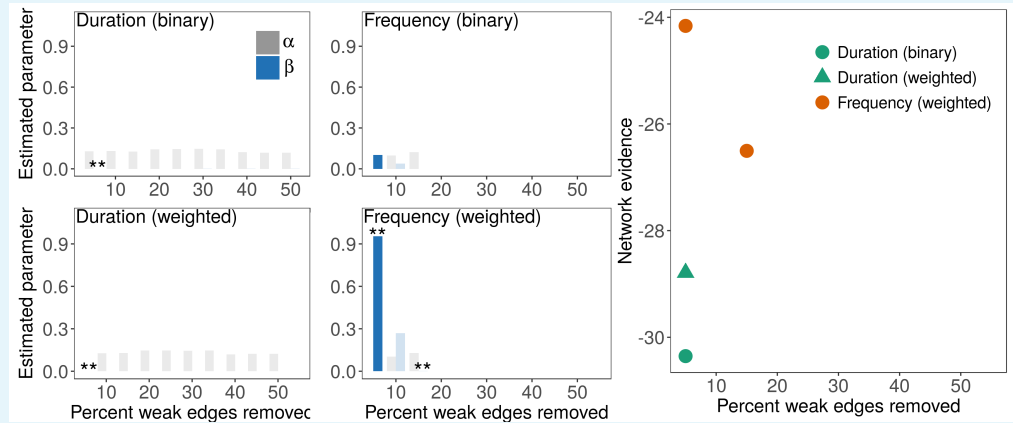
503  
504  
506

**Appendix 1 Figure 1.** Robustness analysis of INoDS on sparse dynamic network with average degree of 2.



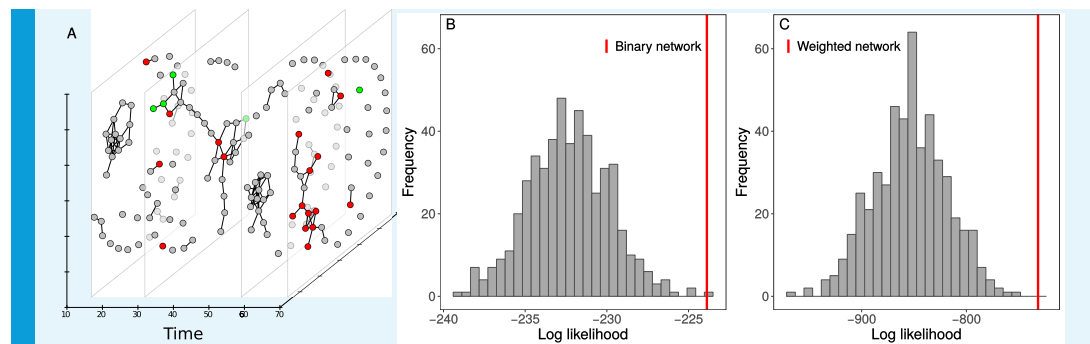
507  
508  
509  
510

**Appendix 1 Figure 2.** Robustness analysis of INoDS,  $k$ -test, and network position test performed on simulated spread of pathogen (SI disease model, transmissibility = 0.03) on *static* network (instead of dynamic network in Fig. 3) with 100 nodes and average degree of 3.



512  
513  
514  
515  
516  
517  
518  
519  
520  
521  
522  
523  
524  
526

**Appendix 1 Figure 3.** Identifying the contact network of *Crithidia* spread in bumble bee colony (colony UN1). (A-D) Edges in the contact network models represent physical interaction between the bees. Since the networks were fully connected, a series of filtered contact networks were constructed by removing weak weighted edges in the network. The x-axis represents the edge-weight threshold that was used to removed weak edges in the network. Two types of edge weights were tested - frequency and duration of contacts. In addition, across all ranges of percent weak edges removed, the two types of weighted network were converted to binary networks. The results shown are estimated values of social transmission parameter  $\beta$ , and estimated values of asocial transmission parameter  $\alpha$ , for the different contact network hypotheses. The darker blue color corresponds to the networks, where the social transmission parameter,  $\beta$  was significantly higher than the asocial transmission parameter,  $\alpha$ . Asterisks (\*\*) indicate significant predictive power of the contact network hypothesis as compared to an ensemble of permuted networks. (E) Log Bayesian (marginal) evidence of the contact networks with high predictive power (i.e., networks marked with asterisks in A-D)



527  
528  
529  
530  
531  
532  
533  
534  
535  
536  
537  
538  
540

**Appendix 1 Figure 4.** Identifying the contact network of *Salmonella* spread Australian sleepy lizards (second site). (A) Dynamic network of proximity interactions between 43 lizards in a population recorded for a total duration of 70 days. Each temporal slice summarizes interaction within a day. Node colors denote the infection status confirmed by laboratory diagnosis. Green nodes are the animals that were diagnosed to be not infected at that time-point, red are the animals that were diagnosis to be infected and grey nodes are the individuals with unknown infection status at time-point. We hypothesized that proximity network with edges that were either binary or weighted with respect to the frequency of interactions could potentially explain the observed spread of *Salmonella* in the population. The predictive power of both (B) binary network ( $P < 0.001$ , log-Bayesian evidence = -766.50) and (C) frequency weighted network ( $P < 0.001$ , log-Bayesian evidence = -255.85) was statistically significant. However, the log Bayes factor of the weighted contact network versus binary contact network, is 510.65, which is a decisive evidence towards the frequency weighted proximity network model.